Eco-Epidemiological Model of Predator-Prey with Two-Strain Infections: The Impact of Herd Behavior

Sanskriti Jain , Balram Dubey , Qian Qian Zheng , Vikas Pandey * , Pankaj Mathur *

Posted Date: 10 October 2024

doi: 10.20944/preprints202410.0819.v1

Keywords: ecology; epidemiology; prey-predator; two strains; herd shape; hopf bifurcation

Article

Eco-Epidemiological Model of Predator-Prey with Two-Strain Infections: The Impact of Herd Behavior

Sanskriti Jain [1], Balram Dubey [2], Q Q Zheng [3], Vikas Pandey [4,5,*] and Pankaj Mathur [1,*]

[1] Department of Mathematics and Astronomy, University of Lucknow, Lucknow, 226007, India
[2] Department of Mathematics, Birla Institute of Technology & Science, Pilani, 333031, Rajasthan. India
[3] School of Science, Xuchang University, Xuchang, 461000, China
[4] Fujita Health University School of Medicine, Toyoake, 470-1192, Japan
[5] RIKEN Center for Brain Science, Saitama, 351-0198, Japan
* Correspondence: pandeyv.ucla@gmail.com (V.P.) ;mathur_p@lkouniv.ac.in (P.M.)

Abstract: This study presents an eco-epidemiological model exploring a prey population infected by two distinct pathogen strains in the presence of an unaffected predator population. The model investigates how prey herding behavior provides protection against predation under multi-strain infections. A well-posedness and boundedness analysis of the populations ensures the robustness of the model. Linear stability analysis reveals that, under specific herd shapes and predator mortality rates, prey infected with either strain can vanish. Bifurcation analysis uncovers critical dynamics: a supercritical Hopf bifurcation occurs at a threshold prey herd shape (k), indicating the onset of stable oscillatory population cycles. As predator mortality (δ) varies, both subcritical and supercritical Hopf bifurcations emerge, marking shifts between stable and unstable dynamics, potentially leading to prey extinction or sharp population collapses. The analysis further identifies a Generalized Hopf bifurcation, distinguishing between predictable cycles and more complex. Numerical simulations confirm these findings, offering insights into predator-prey dynamics in ecosystems subject to multi-strain infections. The results have potential implications for understanding disease control, population stability, and ecological resilience.

Keywords: ecology; epidemiology; prey-predator; two strains; herd shape; hopf bifurcation

1. Introduction

Predator-prey dynamics are critical in maintaining ecological balance, influenced by various factors such as resource availability, environmental conditions, and predation efficiency [1–4]. However, the impact of diseases on these interactions [5–11], especially multi-strain infections [13] within prey populations, has been less explored [14,24–26]. When prey are infected, their ability to evade predators declines, not only due to physical weakening but also through behavioral changes such as the formation of herds. These herds serve as protective mechanisms [21–23,30], but in the presence of infection, they can introduce additional complexity to the predator-prey relationship [12,29,31,32,34].

In this study, we develop an eco-epidemiological model that investigates how two distinct strains of pathogens interact with herding behavior in prey populations, while predators remain unaffected by the infections themselves. This multi-strain dynamic introduces nontrivial challenges in understanding population stability and predator efficiency. Through this model, we explore how herd shape and predator mortality rates, driven by the protective behavior of herds, influence disease dynamics and population survival.

The real-world applicability of this model is significant. Wildlife populations such as deer, wild boars, and fish frequently experience multi-strain infections that affect both prey behavior and predator efficiency [35,36]. Similarly, agricultural systems [39], where livestock herds [37,38] encounter various pathogens, offer another layer of complexity. In marine ecosystems, schooling fish serve as prey for larger predators, where infection can compromise their defense mechanisms [41–43]. Furthermore, urban wildlife and zoonotic diseases [33,47–50] provide an additional domain where multi-strain infections and human interaction complicate traditional predator-prey dynamics [44–46]. The model thus offers critical insights for managing disease outbreaks, ensuring wildlife conservation, and predicting shifts in population stability under varying environmental conditions.

 doi:10.20944/preprints202410.0819.v1

Some researchers have considered two strains of infection either in prey or predator [24–28] but could not show the coexistence of both strains of infections. Martcheva M. [51] considered two types of model with susceptible and two strain infected prey and one with generalist predator, second with specialist predator. She showed that increasing predation leads to eradication of disease without extinction of prey population and also that the presence of specialist predators may lead to the coexistence of both strains. To our knowledge, no one has studied two strains of infection in prey with prey herd and predator mortality due to prey herd. Here we have also assumed both the strains of infections don't affect each other. That means there is neither coinfection nor superinfection,i.e. when an individual species gets infected by one strain, it cannot develop the second strain and have both strains of infection at the same time nor the second strain can replace the first strain.
We focus on analyzing the stability of populations through well-posedness and boundedness evaluations. Using bifurcation analysis, we reveal the critical thresholds at which the prey population undergoes significant dynamic shifts—highlighting the occurrence of supercritical and subcritical Hopf bifurcations, and their roles in population oscillations or collapse. This investigation of bifurcations provides valuable insights into how changes in herd formation or predator mortality due to herd protection can trigger these complex behaviors. We show the presence of the limit point bifurcation of limit cycles, emerging from the Generalized Hopf bifurcation point. This study contributes to a deeper understanding of eco-epidemiological interactions involving multiple infection strains and predator-prey dynamics, laying the groundwork for future models that can incorporate additional environmental and behavioral complexities.

2. Mathematical Model Formulation

The system model is formed based on the following assumptions:

- The susceptible prey grows logistically in the absence of infected prey and predator and prey infected with both strains neither contribute to the reproduction nor to the carrying capacity thus we have,

$$S' = rS(1 - \frac{S}{K}) \tag{1}$$

- Infection of both strains within the prey population occurs horizontally via direct contact following the mass action incidence i.e.

$$H(S, I_j) = \beta_j I_j S \text{ for } j = 1, 2 \tag{2}$$

  where β_j are the rate of transmission of strain j infection.
- Only susceptible prey participates in the herding group where the rate of herd shape is $0 < k < 1$

  1. if the herd shape is circle or square, $k = 0.5$
  2. if the herd shape is cube or sphere, $k = 0.67$.

- The infected prey dies out either due to disease by strain 1 or 2 or naturally (μ_j for $j = 1, 2$ denotes the total death rate)and upon recovery(γ_j for $j = 1, 2$ denotes the recovery rates) from the infection they re-enter the susceptible population.
- Predators attack the susceptible prey according to the Holling-II interaction functional type created by S.Djilali [30] given as

$$H(S, P) = \frac{aS^k P}{1 + ahS^k} \tag{3}$$

  and the prey infected with strains 1 and 2 according to the Holling type-I functional response given as

$$H(I_j, P) = \beta_j I_j P \quad \text{for } j = 1, 2. \tag{4}$$

 doi:10.20944/preprints202410.0819.v1

- Predators attack the boundary of the herd and the prey on the outer herd can injure the predators leading to their death given as $\delta S^k P$.

Using the above postulates, we construct a four-dimensional eco-epidemiological model:

$$\begin{aligned}
\frac{dS}{dt} &= rS\left(1-\frac{S}{K}\right) - [\beta_1 I_1 + \beta_2 I_2]S + \gamma_1 I_1 + \gamma_2 I_2 - \frac{aS^k P}{1+ahS^k} = \phi_1(S, I_1, I_2, P) \\
\frac{dI_1}{dt} &= \beta_1 I_1 S - (\gamma_1 + \mu_1) I_1 - \alpha_1 I_1 P = \phi_2(S, I_1, I_2, P) \\
\frac{dI_2}{dt} &= \beta_2 I_2 S - (\gamma_2 + \mu_2) I_2 - \alpha_2 I_2 P = \phi_3(S, I_1, I_2, P) \\
\frac{dP}{dt} &= \frac{aeS^k P}{1+ahS^k} + e_1\alpha_1 I_1 P + e_2\alpha_2 I_2 P - \delta S^k P - \mu P = \phi_4(S, I_1, I_2, P)
\end{aligned} \tag{5}$$

we have considered a system of equations describing a prey-predator model with two strains of infection running in prey species and prey group forming a herd against the predator.
In the first equation we assume the logistic growth rate of susceptible prey with r as the intrinsic growth rate and K as carrying capacity. The susceptible prey gets infected by strain 1 and strain 2 with rates of transmission β_1, β_2 respectively. The susceptible prey forms a herd and the predator attacks on the boundary of the herd with a Holling type-II interaction functional response.
In the second and third equations, we have the interaction of susceptible prey and the prey infected with strain 1 and strain 2 assuming that the infected can be recovered with rates γ_1, γ_2 and join the class of susceptible prey and die with total death rates μ_1, μ_2 respectively. Also the predator attacks both the prey infected with strain 1 and strain 2 with linear rates α_1, α_2 respectively.
In the fourth equation, we have the growth of predators by consuming susceptible and infected prey with conversion efficiency rates e, e_1, e_2. Also, we have considered the mortality of predators due to prey herd(δ) and their natural death(μ).

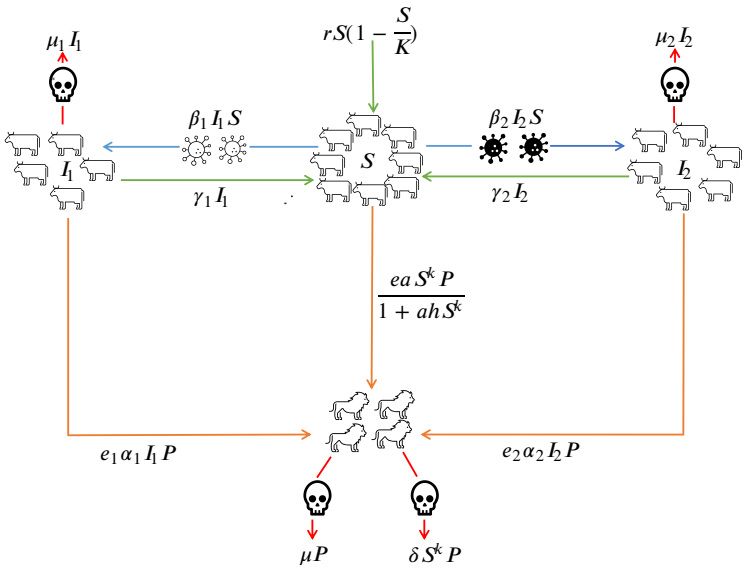

Figure 1. Schematic flowchart for the model.

 doi:10.20944/preprints202410.0819.v1

3. Description of Parameters

Parameters	Description
S	Susceptible Prey
I_1	Prey Infected with strain 1
I_2	Prey Infected with strain 2
P	Predator
r	Intrinsic growth rate of susceptible prey
K	carrying capacity of susceptible prey
β_1	rate of transmission of strain 1 infection
β_2	rate of transmission of strain 2 infection
γ_1	recovery rate from strain 1
γ_2	recovery rate from strain 2
a	rate of predation on susceptible prey
k	rate of prey herd shape
h	handling time spent by a predator on healthy prey
α_1	rate of predation on prey infected with strain 1
α_2	rate of predation on prey infected with strain 2
e	conversion rate of susceptible prey to predator
e_1	conversion rate of prey infected with strain 1 to predator
e_2	conversion rate of prey infected with strain 2 to predator
δ	mortality rate of a predator due to prey herd
μ	natural death rate of predator
μ_1	total death rate of prey infected with strain 1
μ_2	total death rate of prey infected with strain 2

4. Well-Posedness of the Formulated Model

Theorem 1. *All the solutions of the system* (5) *under the given initial condition are unique and positive in R.*

Proof of Theorem 1. The function ϕ_1, ϕ_2, ϕ_3 on the right hand side of system of equation(5) are locally Lipschitz Continuous in the region $\Upsilon = \{(S, I_1, I_2, P) \in [\xi, A] \times [0, B] \times [0, B] \times [0, C]\}$ with ξ a positive real constant. This can be seen $\forall S_1, S_2 \in \Upsilon$ we have,

$$\begin{aligned}
|\phi_1(S_1, I_1, I_2, P) - \phi_1(S_2, I_1, I_2, P)| &\leq r|S_1 - S_2| + \frac{r}{K}|S_1 - S_2||S_1 + S_2| + (\beta_1|I_1| + \beta_2|I_2|)|S_1 - S_2| \\
&+ \frac{a|P||S_1^k - S_2^k||S_1 - S_2|}{|1 + ahS_1^k||1 + ahS_2^k||S_1 - S_2|} \\
&\leq |S_1 - S_2|\left(r + \frac{r(|S_1| + |S_2|)}{K} + \beta_1|I_1| + \beta_2|I_2| \right. \\
&\left. + \frac{a|P|}{|1 + ahS_1^k||1 + ahS_2^k|}\left|\frac{S_1^k - S_2^k}{S_1 - S_2}\right|\right) \\
&\leq L|S_1 - S_2|
\end{aligned}$$

 doi:10.20944/preprints202410.0819.v1

where $L = r + \frac{2rA}{K} + B(\beta_1 + \beta_2) + akCq^{k-1} > 0$ is a Lipschitz constant.
Thus $\phi_1(S, I_1, I_2, P)$ is locally Lipschitz-continuous with respect to S. Similarly, it can be shown for I_1, I_2, P. Hence the system has a unique solution in the region Y.
Now, to show we have positive solutions, we will show $S(t) > 0\ \forall t > 0$ by contradiction. Let us assume there exists a $\tau > 0$ with $\tau = inf\{t : S(t) = 0, t > 0\}$,such that $\frac{dS}{dt}|_{t=\tau} < 0$ and $S(t) > 0\ \forall t \in [0, \tau)$.
From the first equation of (5) we have,

$$\begin{aligned}\left.\frac{dS}{dt}\right|_{t=\tau} &= rS(\tau)\left(1 - \frac{S(\tau)}{K}\right) - [\beta_1 I_1(\tau) + \beta_2 I_2(\tau)]S(\tau) + \gamma_1 I_1\tau) + \gamma_2 I_2(\tau) - \frac{aS^k(\tau)P(\tau)}{1 + ahS^k(\tau)} \\ &= \gamma_1 I_1(\tau) + \gamma_2 I_2(\tau)\end{aligned}$$

we can write the second, third, fourth equations of the model (5) as:
$\frac{dI_1}{dt} = I_1 f_1(S, I_1, I_2, P)$, $\frac{dI_2}{dt} = I_2 f_2(S, I_1, I_2, P)$, $\frac{dP}{dt} = P f_3(S, I_1, I_2, P)$
where
$f_1(S, I_1, I_2, P) = \beta_1 S - \alpha_1 P - \gamma_1 - \mu_1$
$f_2(S, I_1, I_2, P) = \beta_2 S - \alpha_2 P - \gamma_2 - \mu_2$
$f_3(S, I_1, I_2, P) = \frac{eaS^k}{1+ahS^k} + e_1\alpha_1 I_1 + e_2\alpha_2 I_2 - \delta S^k - \mu$
thus it follows,
$I_1(t) = I_1(0)e^{\int_0^t f_1(S(u),I_1(u),I_2(u),P(u))du} \geq 0$
$I_2(t) = I_2(0)e^{\int_0^t f_2(S(u),I_1(u),I_2(u),P(u))du} \geq 0$
$P(t) = P(0)e^{\int_0^t f_3(S(u),I_1(u),I_2(u),P(u))du} \geq 0$
Now we have four cases:
$(1) I_1(0) = I_2(0) = 0$ then
$I_1(t) = I_2(t) = 0\ \forall t > 0 \implies I_1(\tau) = I_2(\tau) = 0$
$\implies \left.\frac{dS}{dt}\right|_{t=\tau} = 0$ which contradicts the condition $\left.\frac{dS}{dt}\right|_{t=\tau} < 0.$
$\implies S(t) > 0\ \forall t \geq 0$
$(2) I_1(0) > 0\ and\ I_2(0) > 0$ then
$I_1(t) > 0\ and\ I_2(t) > 0 \forall t > 0 \implies I_1(\tau) > 0\ and\ I_2(\tau) > 0$
$\implies \left.\frac{dS}{dt}\right|_{t=\tau} > 0$ which contradicts the condition $\left.\frac{dS}{dt}\right|_{t=\tau} < 0.$
$\implies S(t) > 0\ \forall t \geq 0$
Similarly, we can prove for the rest two cases i.e. $I_1(0) = 0, I_2(0) > 0$ and $I_1(0) > 0, I_2(0) = 0$.
Thus all solutions $(S(t), I_1(t), I_2(t), P(t))$ with the stated initial condition remain positive for $\forall t > 0$. □

Theorem 2. *All solutions of the system (5) beginning in R^4_+ stay enclosed in the region* $Y = \{(S, I_1, I_2, P) : 0 < S + I_1 + I_2 \leq \frac{(r+\zeta_1)^2 K}{4r\zeta_1}, 0 < S + \frac{1}{e}P \leq \frac{(r+\zeta_2)^2 K}{4r\zeta_2} + \gamma_1\frac{(r+\zeta_1)^2 K}{4r\zeta_1\zeta_2} + \gamma_2\frac{(r+\zeta_1)^2 K}{4r\zeta_1\zeta_2}$, *where $\zeta_1$and ζ_2 are some real numbers satisfying* $0 < \zeta_1 < min\{\mu_1, \mu_2\}, 0 < \zeta_2 < \mu - \frac{(e_1\alpha_1 + e_2\alpha_2)(r+\zeta_1)^2 K}{4r\zeta_1}$

 doi:10.20944/preprints202410.0819.v1

Proof of Theorem 2. From the first equation of the system, we have $\limsup_{t\to\infty} S(t) \leq K$.
Let $\phi_1 = S + I_1 + I_2$ and $\zeta_1 > 0$. Then

$$\begin{aligned}\frac{d\phi_1}{dt} + \zeta_1\phi_1 &= rS(1-\frac{S}{K}) - \frac{aS^kP}{1+ahS^k} - \alpha_1 I_1 P - \alpha_2 I_2 P - \mu_1 I_1 - \mu_2 I_2 + \zeta_1(S + I_1 + I_2)\\ &\leq rS(1-\frac{S}{K}) - \mu_1 I_1 - \mu_2 I_2 + \zeta_1(S + I_1 + I_2)\\ &\leq (r+\zeta_1)S - \frac{rS^2}{K} - (\mu_1 - \zeta_1)I_1 - (\mu_2 - \zeta_1)I_2\\ &\leq (r+\zeta_1)S - \frac{rS^2}{K}, \text{for } \zeta_1 < min\{\mu_1, \mu_2\}\end{aligned}$$

since $\max_{S\geq 0}(r+\zeta_1)S - \frac{rS^2}{K} = \frac{(r+\zeta_1)^2K}{4r}$.
Therefore, $\frac{d\phi_1}{dt} + \zeta_1\phi_1 \leq \frac{(r+\zeta_1)^2K}{4r} \implies \limsup_{t\to\infty}(S(t) + I_1(t) + I_2(t)) \leq \frac{(r+\zeta_1)^2K}{4r\zeta_1}$.

Now, to check boundedness of $P(t)$ we assume $\phi_2 = S + \frac{1}{e}P$ and $\zeta_2 > 0$. Then

$$\begin{aligned}\frac{d\phi_2}{dt} + \zeta_2\phi_2 &= rS(1-\frac{S}{K}) - \beta_1 I_1 S - \beta_2 I_2 S + \gamma_1 I_1 + \gamma_2 I_2 + \frac{e_1}{e}\alpha_1 I_1 P + \frac{e_2}{e}\alpha_2 I_2 P\\ &\quad - \frac{\delta}{e}S^kP - \frac{\mu}{e}P + \zeta_2 S + \frac{\zeta_2}{e}P\\ &\leq (r+\zeta_2)S - \frac{rS^2}{K} + \gamma_1 I_{1max} + \gamma_2 I_{2max} - (\frac{\mu}{e} - \frac{\zeta_2}{e} - \frac{e_1}{e}\alpha_1 I_{1max} - \frac{e_2}{e}\alpha_2 I_{2max})P\end{aligned}$$

where $I_{1max} = I_{2max} = \frac{(r+\zeta_1)^2K}{4r\zeta_1}$.

Now for $0 < \zeta_2 < \mu - e_1\alpha_1 I_{1max} - e_2\alpha_2 I_{2max}$, we have

$\frac{d\phi_2}{dt} + \zeta_2\phi_2 \leq (r+\zeta_2)S - \frac{rS^2}{K} + \gamma_1 I_{1max} + \gamma_2 I_{2max}$

which implies $\limsup_{t\to\infty}(S(t) + \frac{1}{e}P(t)) \leq \frac{(r+\zeta_2)^2K}{4r\zeta_2} + \gamma_1\frac{(r+\zeta_1)^2K}{4r\zeta_1\zeta_2} + \gamma_2\frac{(r+\zeta_1)^2K}{4r\zeta_1\zeta_2}$.
Hence the theorem follows. □

5. Equilibrium Points

The model system (5) has following feasible equilibrium points:

1. $E_1 = (0,0,0,0)$
2. $E_2 = (K,0,0,0)$
   The basic reproduction number at the disease-free equilibrium point is
   $R_0 = max\{R_0^1, R_0^2\}$ where $R_0^1 = \frac{\beta_1 K}{\gamma_1+\mu_1}, R_0^2 = \frac{\beta_2 K}{\gamma_2+\mu_2}$
3. $E_3 = (S_{SP}, 0, 0, P_{SP})$
   where S_{SP} and P_{SP} are solutions of equations:
   $ah\delta S^{2k} + S^k(\delta + \mu ah - ae) + \mu = 0$ and $rS(1-\frac{S}{K}) - \frac{aS^kP}{1+ahS^k} = 0$
   For positive solutions, the following conditions should hold:
   $(\mu ah + \delta - ae)^2 \geq 4ah\delta\mu$ and $\delta + \mu ah < ae$
4. $E_4 = (S_1, I_1, 0, 0)$
   where $S = \frac{\mu_1+\gamma_1}{\beta_1}, I_1 = \frac{rS}{\mu_1}(1-\frac{S}{K})$
5. $E_5 = (S_2, 0, I_2, 0)$
   where $S = \frac{\mu_2+\gamma_2}{\beta_2}, I_2 = \frac{rS}{\mu_2}(1-\frac{S}{K})$

 doi:10.20944/preprints202410.0819.v1

6. $E_6 = (S_{I_1P}, I_1, 0, P)$
   where $I_1 = \frac{1}{e_1\alpha_1}\left(\delta S^k + \mu - \frac{eaS^k}{1+ahS^k}\right)$, $P = \frac{\beta_1 S - \gamma_1 - \mu_1}{\alpha_1}$
   $f_1(S) = A_1S^{2k+1} + A_2S^{2k} + A_3S^{k+2} + A_4S^{k+1} + A_5S^k + A_6S^2 + A_7S + A_8$

   where $A_1 = \delta ahK\beta_1, A_2 = -\delta ah\gamma_1 K, A_3 = ahre_1\alpha_1, A_4 = \beta_1 e_1 aK - aeK\beta_1 + K\beta_1\delta + \mu ahK\beta_1 - re_1\alpha_1 ahK,$
   $A_5 = ae\gamma_1 K - \delta\gamma_1 K - \mu ah\gamma_1 K - (\gamma_1 + \mu_1)e_1 aK, A_6 = re_1\alpha_1, A_7 = K(\mu\beta_1 - re_1\alpha_1), A_8 = -\mu\gamma_1 K$

7. $E_7 = (S_{I_2P}, 0, I_2, P)$
   where $I_1 = \frac{1}{e_2\alpha_2}(\delta S^k + \mu - \frac{eaS^k}{1+ahS^k})$, $P = \frac{\beta_2 S - \gamma_2 - \mu_2}{\alpha_2}$
   $f_2(S) = A_1S^{2k+1} + A_2S^{2k} + A_3S^{k+2} + A_4S^{k+1} + A_5S^k + A_6S^2 + A_7S + A_8$

   where $A_1 = \delta ahK\beta_2, A_2 = -\delta ah\gamma_2 K, A_3 = ahre_2\alpha_2, A_4 = \beta_2 e_2 aK - aeK\beta_2 + K\beta_2\delta + \mu ahK\beta_2 - re_2\alpha_2 ahK,$
   $A_5 = ae\gamma_2 K - \delta\gamma_2 K - \mu ah\gamma_2 K - (\gamma_2 + \mu_2)e_2 aK, A_6 = re_2\alpha_2, A_7 = K(\mu\beta_2 - re_2\alpha_2), A_8 = -\mu\gamma_2 K.$

8. $E^* = (S^*, I_1^*, I_2^*, P^*)$ where $P^* = \frac{\beta_1 S - \mu_1 - \gamma_1}{\alpha_1} = \frac{\beta_2 S - \mu_2 - \gamma_2}{\alpha_2}$
   $\implies S^* = \frac{\alpha_2(\mu_1+\gamma_1) - \alpha_1(\mu_2+\gamma_2)}{\beta_1\alpha_2 - \alpha_1\beta_2}$

$$I_1^* = \frac{K\alpha_1(\gamma_2 - \beta_2 S)(\delta S^k + \mu + ah\delta S^{2k} + \mu ahS^k - aeS^k) - e_2\alpha_2(\beta_1 aKS^{k+1}) + e_2\alpha_2(\mu_1 + \gamma_1)KaS^k + e_2\alpha_2\alpha_1 rS(1+ahS^k)(K-S)}{K\alpha_1(1+ahS^k)(e_1\alpha_1(\gamma_2 - \beta_2 S) - e_2\alpha_2(\gamma_1 - \beta_1 S))}$$

$$I_2^* = \frac{K\alpha_1(\gamma_1 - \beta_1 S)(\delta S^k + \mu + ah\delta S^{2k} + \mu ahS^k - aeS^k) - e_1\alpha_1(\beta_1 aKS^{k+1}) + e_1\alpha_1(\mu_1 + \gamma_1)KaS^k + e_1\alpha_1^2 rS(1+ahS^k)(K-S)}{K\alpha_1(1+ahS^k)(e_2\alpha_2(\gamma_1 - \beta_1 S) - e_1\alpha_1(\gamma_2 - \beta_2 S))}$$

6. Stability Conditions

1. $E_1(0,0,0,0)$ is a saddle point because the eigenvalues of variational matrix are $(r, -\gamma_1 - \mu_1, -\gamma_2 - \mu_2, -m)$
2. $E_2(K,0,0,0)$ is locally asymptotically stable if $\frac{K^k ae}{K^k ah+1} < K^k d + m$ and $K\beta_1 < \mu_1 + \gamma_1$ and $K\beta_2 < \mu_2 + \gamma_2$
3. for E^* the variational matrix is

$$J = \begin{bmatrix} J_{11} & J_{12} & J_{13} & J_{14} \\ J_{21} & J_{22} & J_{23} & J_{24} \\ J_{31} & J_{32} & J_{33} & J_{34} \\ J_{41} & J_{42} & J_{43} & J_{44} \end{bmatrix}$$

where $J_{11} = \frac{a^2 hkS^{*(2k-1)}P^*}{(1+ahS^{*k})^2} - \beta_2 I_2^* + r(1 - \frac{S^*}{K}) - \frac{rS^*}{K} - \frac{akS^{*(k-1)}P^*}{1+ahS^{*k}} - \beta_1 I_1^*$
$J_{12} = \gamma_1 - \beta_1 S^*, J_{13} = \gamma_2 - \beta_2 S^*, J_{14} = -\frac{aS^{*k}}{1+ahS^{*k}}$
$J_{21} = \beta_1 I_1^*, J_{22} = \beta_1 S^* - \mu_1 - \alpha_1 P^* - \gamma_1, J_{23} = 0, J_{24} = -\alpha_1 I_1^*$
$J_{31} = \beta_2 I_2^*, J_{32} = 0, J_{33} = \beta_2 S^* - \mu_2 - \alpha_2 P^* - \gamma_2, J_{34} = -\alpha_2 I_2^*$
$J_{41} = \frac{aekS^{*(k-1)}P^*}{1+ahS^{*k}} - dkS^{*(k-1)}P^* - \frac{a^2 ehkS^{*(2k-1)}P^*}{(1+ahS^{*k})^2}$
$J_{42} = \alpha_1 e_1 P^*, J_{43} = \alpha_2 e_2 P^*$
$J_{44} = \alpha_1 e_1 I_1^* - dS^{*k} - m + \alpha_2 e_2 I_2^* + \frac{aeS^{*k}}{1+ahS^{*k}}$
The characteristic polynomial of matrix J is

$$\lambda^4 + a_1\lambda^3 + a_2\lambda^2 + a_3\lambda + a_4 = 0 \tag{6}$$

 doi:10.20944/preprints202410.0819.v1

where

$$
\begin{aligned}
a_1 &= -(J_{11} + J_{22} + J_{33} + J_{44}) \\
a_2 &= J_{11}J_{22} - J_{12}J_{21} + J_{11}J_{33} - J_{13}J_{31} + J_{11}J_{44} - J_{14}J_{41} + J_{22}J_{33} - J_{23}J_{32} + J_{22}J_{44} - J_{24}J_{42} + J_{33}J_{44} - J_{34}J_{43} \\
a_3 &= J_{11}J_{23}J_{32} - J_{11}J_{22}J_{33} + J_{12}J_{21}J_{33} - J_{12}J_{23}J_{31} - J_{13}J_{21}J_{32} + J_{13}J_{22}J_{31} - J_{11}J_{22}J_{44} + J_{11}J_{24}J_{42} + J_{12}J_{21}J_{44} \\
&\quad - J_{12}J_{24}J_{41} - J_{14}J_{21}J_{42} + J_{14}J_{22}J_{41} - J_{11}J_{33}J_{44} + J_{11}J_{34}J_{43} + J_{13}J_{31}J_{44} - J_{13}J_{34}J_{41} - J_{14}J_{31}J_{43} + J_{14}J_{33}J_{41} \\
&\quad - J_{22}J_{33}J_{44} + J_{22}J_{34}J_{43} + J_{23}J_{32}J_{44} - J_{23}J_{34}J_{42} - J_{24}J_{32}J_{43} + J_{24}J_{33}J_{42} \\
a_4 &= J_{11}J_{22}J_{33}J_{44} - J_{11}J_{22}J_{34}J_{43} - J_{11}J_{23}J_{32}J_{44} + J_{11}J_{23}J_{34}J_{42} + J_{11}J_{24}J_{32}J_{43} - J_{11}J_{24}J_{33}J_{42} - J_{12}J_{21}J_{33}J_{44} \\
&\quad + J_{12}J_{21}J_{34}J_{43} + J_{12}J_{23}J_{31}J_{44} - J_{12}J_{23}J_{34}J_{41} - J_{12}J_{24}J_{31}J_{43} + J_{12}J_{24}J_{33}J_{41} + J_{13}J_{21}J_{32}J_{44} - J_{13}J_{21}J_{34}J_{42} \\
&\quad - J_{13}J_{22}J_{31}J_{44} + J_{13}J_{22}J_{34}J_{41} + J_{13}J_{24}J_{31}J_{42} - J_{13}J_{24}J_{32}J_{41} - J_{14}J_{21}J_{32}J_{43} + J_{14}J_{21}J_{33}J_{42} + J_{14}J_{22}J_{31}J_{43} \\
&\quad - J_{14}J_{22}J_{33}J_{41} - J_{14}J_{23}J_{31}J_{42} + J_{14}J_{23}J_{32}J_{41}
\end{aligned}
$$

According to Routh-Hurwitz criteria E^* is locally asymptotically stable if and only if
$\mathbf{a_1 > 0, a_4 > 0, a_1a_2 - a_3 > 0, a_1a_2a_3 - a_3^2 - a_4a_1^2 > 0}$

Theorem 3. *The necessary and sufficient conditions for Hopf bifurcation to occur at E^* at $k = k^*$ are the following:*

- $a_1 > 0, a_4 > 0, a_1a_2 - a_3 > 0$
- $a_1a_2a_3 - a_3^2 - a_4a_1^2 = 0$
- $a_1^2(k^*)(a_2(k^*)'a_3(k^*) + a_2(k^*)a_3'(k^*) - a_4'(k^*)a_1(k^*)) - 2a_3(k^*)a_3'(k^*)a_1(k^*)$
  $+ a_1'(k^*)(a_2(k^*)a_3(k^*)a_1(k^*) + 2a_3^2(k^*)) \neq 0$

Proof of Theorem 3. At $k = k^*$ the characteristic equation (6)becomes

$$\left(\lambda^2(k) + \frac{a_3(k)}{a_1(k)}\right)(\lambda(k) + x_1(k))(\lambda(k) + x_2(k)) = 0 \tag{7}$$

where $x_1 + x_2 = a_1, x_1x_2 = a_2 - \frac{a_3}{a_1}$
Now to show the transversality condition for Hopf-bifurcation. Let us assume $\lambda(k) = u(k) + iv(k)$. Substituting this in (7) we have,

$$D(k)u(k)' - E(k)v(k)' + G(k) = 0 \tag{8}$$
$$E(k)u(k)' + D(k)v(k)' + H(k) = 0 \tag{9}$$

where

$$
\begin{aligned}
D(k) &= 4u^3(k) - 12u(k)v^2(k) + 3u^2(k)a_1(k) - 3a_1(k)v^2(k) + 2a_2(k)u(k) + a_3(k) \\
E(k) &= 12u^2(k)v(k) - 4v^3(k) + 6u(k)v(k)a_1(k) + 2a_2(k)v(k) \\
G(k) &= a_1'(k)(u^3(k) - 3u(k)v^2(k)) + a_2'(k)(u^2(k) - v^2(k)) + a_3'(k)u(k) + a_4'(k) \\
H(k) &= a_1'(k)(3u^2(k)v(k) - v^3(k)) + a_3'(k)v(k) + 2a_2'(k)u(k)v(k)
\end{aligned}
$$

 doi:10.20944/preprints202410.0819.v1

Now at $k = k^*$, $\quad u(k^*) = 0, v(k^*) = \sqrt{\frac{a_3}{a_1}}$
Hence we have,

$$D(k^*) = a_3(k^*) - 3a_1(k^*)v^2(k^*) = -2a_3(k^*)$$
$$E(k^*) = 2a_2(k^*)v(k^*) - 4v^3(k^*) = 2v(k^*)\left(a_2(k^*) - 2\frac{a_3(k^*)}{a_1(k^*)}\right)$$
$$G(k^*) = a_4'(k^*) - a_2'(k^*)v^2(k^*) = a_4'(k^*) - a_2'(k^*)\frac{a_3(k^*)}{a_1(k^*)}$$
$$H(k^*) = a_3'(k^*)v(k^*) - v^3(k^*)a_1'(k^*) = v(k^*)\left(a_3'(k^*) - a_1'(k^*)\frac{a_3(k^*)}{a_1(k^*)}\right)$$

On solving (8) and (9) using Cramer's rule for $u'(k^*)$ we get

$$\begin{aligned}\left[\frac{dRe(\lambda(k))}{dk}\right]_{k=k^*} &= u'(k^*)\\ &= -\frac{G(k^*)D(k^*) + H(k^*)E(k^*)}{D^2(k^*) + E^2(k^*)}\\ &= -\frac{2a_3(k^*)}{a_1(k^*)}\frac{M}{D^2(k^*) + E^2(k^*)} \neq 0\end{aligned}$$

provided $M \neq 0$ where
$M = a_1^2(k^*)(a_2(k^*)'a_3(k^*) + a_2(k^*)a_3'(k^*) - a_4'(k^*)a_1(k^*)) - 2a_3(k^*)a_3'(k^*)a_1(k^*)$
$+ a_1'(k^*)(a_2(k^*)a_3(k^*)a_1(k^*) + 2a_3^2(k^*))$

Hence the theorem follows. □

7. Numerical Simulation

We first search the equilibrium conditions at parameter values given in the Table 1. The corresponding interior equilibrium point $E^* = (16.1282, 3.1825, 0.9785, 0.3282)$ with eigenvalues $(-0.0036 \pm 0.2189i, -0.0754, -0.0132)$. We have focused on the behavior of two types of infection within the prey population. First, we show the time series of the two infections under consideration in Figure 2 for the homogeneous distribution of the prey, which shows there is no impact of the herd here. However, we observe that due to the higher recovery and death rates of infection I_1 compared to I_2, the prevalence of I_1 decays sharply. Consequently, the other variables also stabilize, reaching a steady state. A similar behavior can be expected if the recovery and death rates of I_2 were higher than those of I_1.
(a) **Effect of prey herd shape(k)**: At $k = 1$, the prey distribution is homogeneous. The value of k reflects the herd shape of the prey, with higher values corresponding to more structured forms, such as cubes or spheres. For instance, $k = 0.67$ represents a more defined shape like a sphere or cube, while $k = 0.5$ depicts a 2D circular or square herd configuration. Figure 3 illustrates the occurrence of a Hopf bifurcation within this parameter space at $k = 0.722467$, keeping all the other parameters as in Table 1. The first Lyapunov coefficient(FLC) at this point is -1.914324×10^{-4} which is negative thus confirming supercritical Hopf bifurcation. For the bifurcation analysis a numerical continuation bifurcation package MatCont has been used [52]. The periodic oscillations in the predator populations show that for lower values of k, the predator population decreases. As we increase the value of k, the population decay slows and eventually reaches stable limit cycles at the Hopf bifurcation point. However, we can observe a switching mechanism in the prey population with respect to strain 1. When I_1 is high, I_2 is low, and vice versa. Therefore, as I_2 decays during oscillations, I_1 increases and then decays, but eventually stabilizes at a higher value, while the I_2 infection dies out over time.

 doi:10.20944/preprints202410.0819.v1

Table 1. Parameter Description.

Parameters	Numerical Values	Source
r	0.15	Assumed
K	25	Assumed
β_1	0.01	[13]
β_2	0.02	[13]
γ_1	0.03	[13]
γ_2	0.01	Assumed
a	0.5	[12]
k	0.55	[12]
h	2	[12]
α_1	0.15625	Assumed
α_2	0.8	Assumed
e	0.85	[12]
e_1	0.17	[12]
e_2	0.17	[12]
δ	0.0145	[12]
μ	0.5	[12]
μ_1	0.08	Assumed
μ_2	0.05	[12]

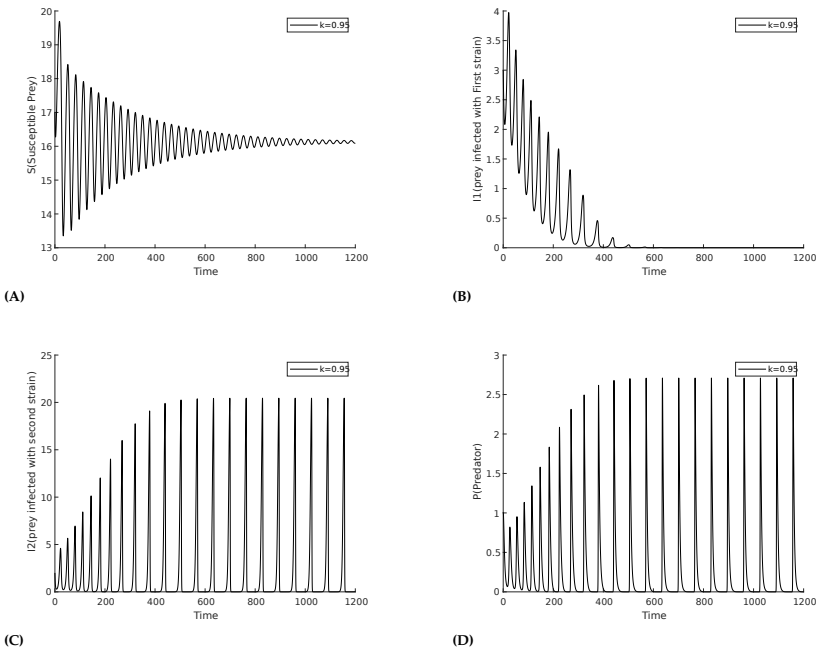

Figure 2. Time series plot depicting the decline of (B) prey infected with strain 1, alongside other variables: (A) Susceptible prey, (C) prey infected with strain 2, (D) Predator population.

 doi:10.20944/preprints202410.0819.v1

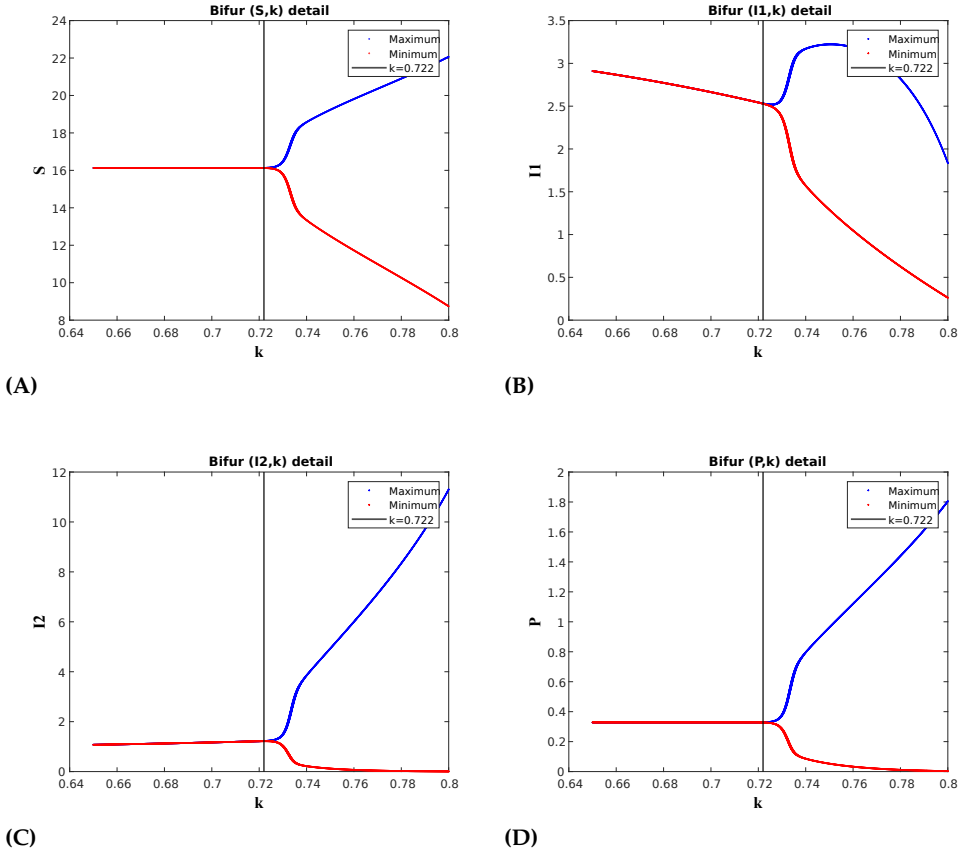

Figure 3. The Hopf-bifurcation diagram for k shows the onset of periodic oscillations following the bifurcation point at $k = k^* = 0.722$. In the diagram, red and blue colors indicate the maximum and minimum values of the positive solution during the steady-state phase, respectively. For values of k less than k^*, the convergence of the maximum and minimum values indicates the stability of E^*. Beyond this point, the solution begins to oscillate between these maximum and minimum values, indicating a loss of stability.

As we have observed the supercritical Hopf bifurcation, we attempt to identify the subcritical Hopf bifurcation in the $k - e_1$ parametric space. The occurrence of a subcritical Hopf bifurcation is particularly interesting due to the existence of an unstable limit cycle within the linearly stable region [15–20]. The demarcation point between the subcritical and supercritical Hopf bifurcations is the Generalized Hopf bifurcation point, which can be reached through the simultaneous variation of two parameters like $k - e_1$ here. In Figure 5, we have identified the Generalized Hopf bifurcation which is a codimension-2 bifurcation of fixed point, from which a limit point bifurcation of the limit cycle curve (LPC curve) emerges. In this bifurcation, the unstable limit cycle folds into a stable limit cycle of higher amplitude. This LPC curve is also referred to as the global stability boundary by Pandey et al. [15,16] (b)**Effect of death of predator due to prey herd(δ)**: In figure 6, the parameter δ represents the rate of predator mortality due to the herd effect, and we also observe a Hopf bifurcation on this parameter at $\delta = \delta^* = 0.0296$ where the First Lyapunov coefficient(FLC) is -1.364586×10^{-4} which is negative thus showing Supercritical Hopf bifurcation. At $\delta = \delta^{**} = 0.0207$, we have a Hopf point with First Lyapunov Coefficient 2.085063×10^{-4} which is positive thus confirming subcritical Hopf bifurcation. For an increased death rate of the predator, the oscillation amplitude of I_1 becomes very low because there are fewer predators to attack each population. As a result, due to the high recovery and death rates, I_1 diminishes to zero.

 doi:10.20944/preprints202410.0819.v1

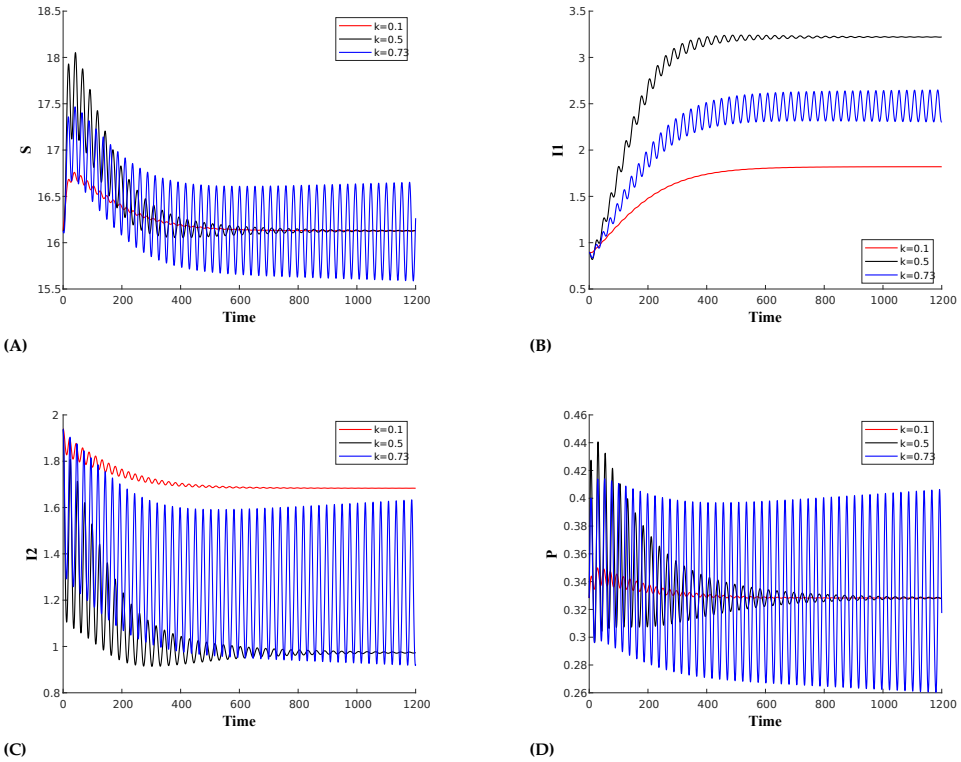

Figure 4. The time series plot for the Supercritical Hopf bifurcation showing the influence of the prey herd shape (k) on : (A) Susceptible prey,(B) prey infected with strain 1, (C) prey infected with strain 2, (D) Predator population.

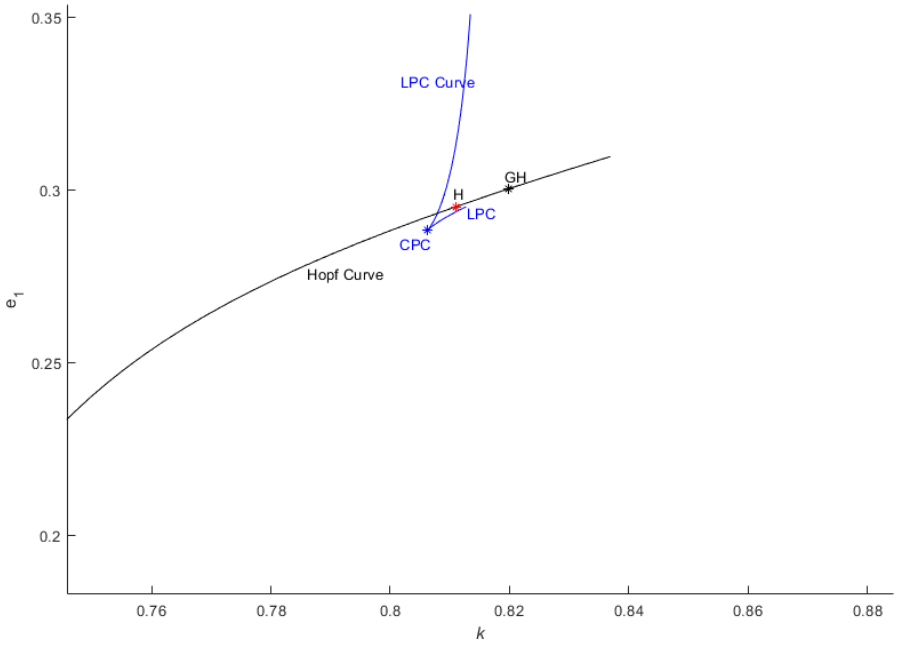

Figure 5. Hopf curve for $k - e_1$ parametric space where GH represents Generalized Hopf point.

We demonstrate that the oscillation amplitude of I_1 is very low for higher values of δ, as shown in Figure 6b. Furthermore, a switching mechanism is observed between I_1 and I_2. In Figure 7, for $\delta = 0.018$, I_1 is higher while I_2 is dying, and for $\delta = 0.028$, I_1 declines while I_2 becomes more prominent.

 doi:10.20944/preprints202410.0819.v1

However, oscillations are still present for higher values of δ, though with a reduced amplitude due to the limited number of predators attacking each population. Figure 8 shows that only one infection survives, as I_1 dies, while the I_2 shows the growing oscillations for higher value of δ.

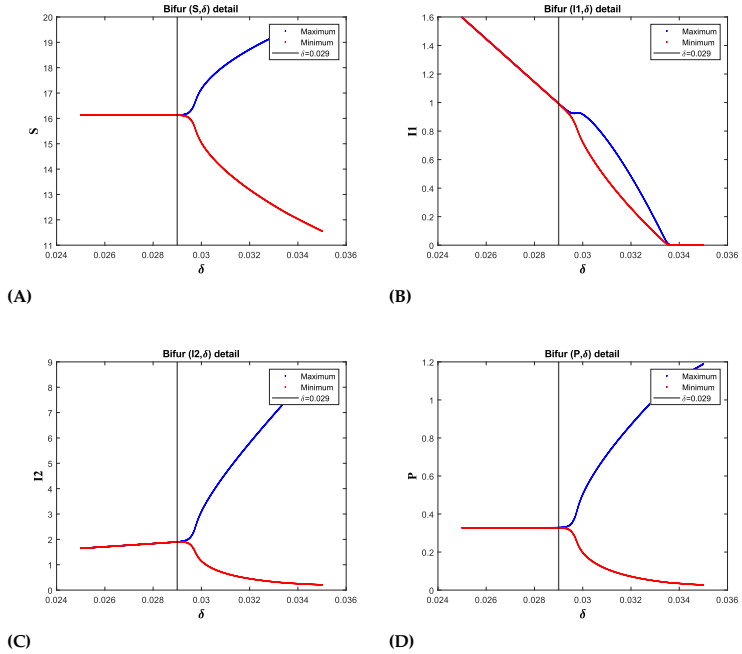

Figure 6. The Supercritical Hopf-bifurcation diagram for δ shows the onset of periodic oscillations following the bifurcation point at $\delta = \delta^* = 0.0296$. In the diagram, red and blue colors indicate the maximum and minimum values of the positive solution during the steady-state phase, respectively. For values of δ less than δ^*, the convergence of the maximum and minimum values indicates the stability of E^*. Beyond this point, the solution begins to oscillate between these maximum and minimum values, indicating a loss of stability.

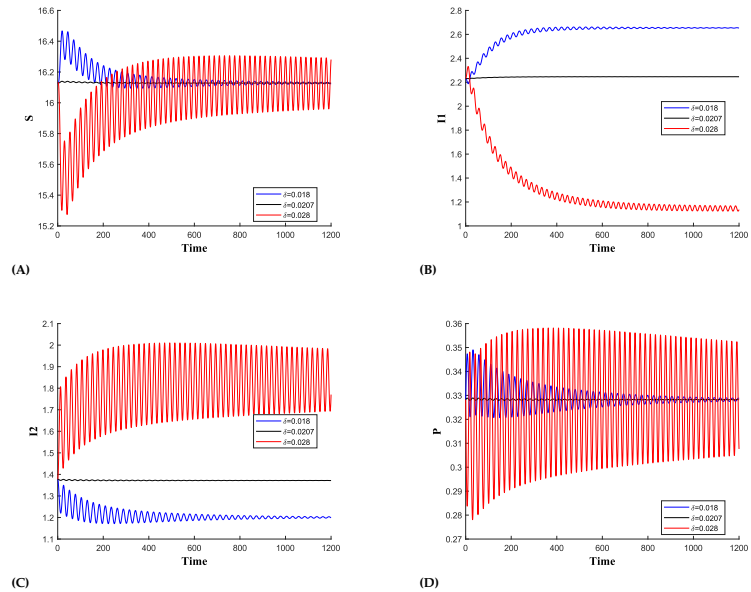

Figure 7. The time series plot for the Subcritical hopf bifurcation showing the influence of the predator mortality due to prey herd (δ) on: (A) Susceptible prey,(B) prey infected with strain 1, (C) prey infected with strain 2, (D) Predator population

 doi:10.20944/preprints202410.0819.v1

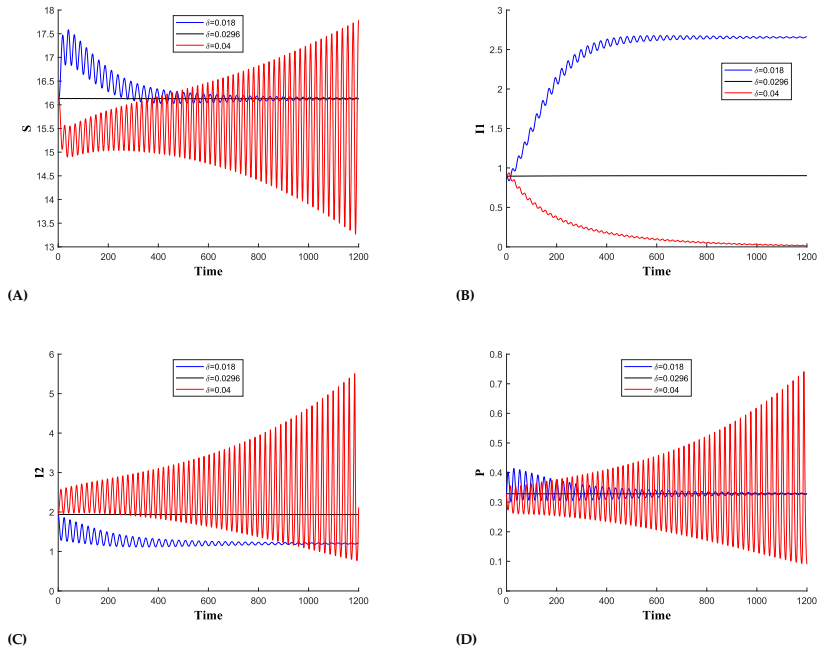

Figure 8. The time series plot for the Supercritical hopf bifurcation showing the influence of the predator mortality due to prey herd (δ) on: (A) Susceptible prey,(B) prey infected with strain 1, (C) prey infected with strain 2, (D) Predator population

8. Conclusions

In this article, we studied the dynamics of two strains of infection in the prey population. The disease transmission is not vertical,i.e. not transferable to offspring. The susceptible prey is assumed to form a herd against predators. In 2D, prey herd for a circle or square is 0.5, and in 3D, for a sphere, it is 0.67. We have generalized the rate of prey herd between 0 and 1. Also, we have assumed predator mortality due to prey herd. According to [21], prey on the circumference of the herd can injure predators. The presented model is well-posed and all the solutions are positive and bounded. We identified the biologically feasible equilibrium points and discussed the stability criteria for the interior equilibrium point where all populations coexist. Further, it was observed that the ecosystem cannot disappear since the trivial equilibrium point $E_1(0,0,0,0)$ is a saddle point i.e. inherently unstable which is a positive point for the given model. We also show the only healthy prey equilibrium point $E_2(K,0,0,0)$ is locally asymptotically stable under certain conditions and if the basic reproduction number $R_0 < 1$. If $R_0^1 > 1$ then prey infected with the first strain will dominate and if $R_0^2 > 1$ then prey infected with the second strain will dominate. Elena et al. [24,25] analyzed two different types of models with two strains of infection in the prey population. Their mathematical findings display no coexistence with both disease strains. Similarly, Roman et al. [26] considered two strain infections in predators, Bosica et al. [27] considered two strain infections in prey with mutualism but could not establish coexistence of equilibrium with both disease strains. However, our work shows the existence of an interior equilibrium point $E^*(S^*, I_1^*, I_2^*, P^*)$ where both the infections coexist. In Figure 3 we detected a supercritical hopf bifurcation about E^* for prey herd shape $k = 0.722467$. Gupta and Dubey [12] observed a resembling situation for $k = 0.6621$ in the case of one infection strain. Moreover, in Figure 2 our research reveals that for a particular herd shape at $k = 0.950245$ prey infected with strain 1 dies and other populations settle to a stable limit cycle. Further investigations demonstrate changes in population on increasing the mortality rate(δ) of predators due to prey herd. It is observed in Figure 6, that at $\delta = 0.0296$ system undergoes supercritical Hopf bifurcation and a stable limit cycle bifurcates. In addition to this, it is seen in Figure 8, for high values of δ (say= 0.04) prey infected with strain 1 dies out. Further, in the model we have detected significant bifurcation phenomena, consisting of the generalized Hopf bifurcation, the cusp point, and the limit point of cycles (LPC) curve. However, a

 doi:10.20944/preprints202410.0819.v1

detailed analysis and extensive investigation of these bifurcations, including their biological inferences and further understanding of the system's dynamics, will be attended in future work. These factors hold significant prospects in understanding the complex interplay between spread of infection and population dynamics and will form the basis of later studies.

Author Contributions: Conceptualization, V.P. and B.D.; methodology, S.J.; software, S.J.; validation, S.J. and V.P.; formal analysis, S.J. and P.M.; investigation, S.J.; resources, P.M. and V.P. and B.D.; data curation, S.J.; writing—original draft preparation, S.J., B.D., Q.Z., V.P. and P.M.; writing—review and editing,S.J., B.D., Q.Z., V.P. and P.M.; visualization, V.P. and B.D.; supervision, V.P. and P.M.; project administration, V.P.; funding acquisition, P.M. and V.P. All authors have read and agreed to the published version of the manuscript.

Funding: This research received no external funding.

Conflicts of Interest: The authors declare no conflicts of interest.

References

1. Upadhyay, R.K.; Iyengar, S.R. K.; Rai, V. Chaos: an ecological reality? *International Journal of Bifurcation and Chaos* **1998**,*08*, 1325–1333. https://doi.org/10.1142/s0218127498001029
2. Aziz-Alaoui, M. Study of a Leslie–Gower-type tritrophic population model. *Chaos Solitons & Fractals* **2022**, *14*, 1275–1293. https://doi.org/10.1016/s0960-0779(02)00079-6
3. Verma, H.; Antwi-Fordjour, K.; Hossain, M.; Pal, N.; Parshad, R.D.; Mathur, P. A "Double" fear effect in a tri-trophic food chain model. *The European Physical Journal Plus* **2021**, *136*.
4. Verma, H.; Mathur, P. Analysis of chaotic situation in three species food chain model. *Ganita* **2019**, *69*, 57–65.
5. Garai, S.; Hossain, M.; Karmakar, S.; Pal, N. Chaos, periodic structures, and multistability: Complex dynamical behaviors of an eco-epidemiological model in parameter planes.*Chaos an Interdisciplinary Journal of Nonlinear Science* **2023**, *33*. https://doi.org/10.1063/5.0156110
6. Jana, S.; Kar, T. Modeling and analysis of a prey–predator system with disease in the prey. *Chaos Solitons & Fractals* **2013**, *47*, 42–53.https://doi.org/10.1016/j.chaos.2012.12.002
7. Chattopadhyay, J.; Srinivasu, P.; Bairagi, N. Pelicans at risk in Salton sea — an eco-epidemiological model. *Ecological Modelling* **2001**, *136*, 103–112. https://doi.org/10.1016/s0304-3800(00)00350-1
8. Gupta, A.; Dubey, B. Bifurcations and multi-stability in an eco-epidemic model with additional food. *The European Physical Journal Plus* **2022**, *137*.https://doi.org/10.1140/epjp/s13360-022-02340-3
9. Upadhyay, R. K.; Roy, P. Spread of a disease and its effect on population dynamics in an eco-epidemiological system. *Communications in Nonlinear Science and Numerical Simulation* **2014**, *19*, 4170–4184.https://doi.org/10.1016/j.cnsns.2014.04.016
10. Ghosh, M.; Li, X.Z. Mathematical modelling of prey-predator interaction with disease in prey.*International Journal of Computing Science and Mathematics* **2016**, *7*, 443. https://doi.org/10.1504/ijcsm.2016.080075
11. Chattopadhyay, J.; Arino, O. A predator-prey model with disease in the prey.*Nonlinear Analysis* **1999**, *36*, 747–766. https://doi.org/10.1016/s0362-546x(98)00126-6
12. Gupta, A.; Dubey, B. Bifurcation and chaos in a delayed eco-epidemic model induced by prey configuration.*Chaos Solitons & Fractals* **2022**, *165*, 112785.https://doi.org/10.1016/j.chaos.2022.112785
13. Lazebnik, T.; Bunimovich-Mendrazitsky, S. Generic approach for mathematical model of multi-strain pandemics. *PloS One* **2022**, *17*, e0260683. https://doi.org/10.1371/journal.pone.0260683
14. Alexi, A.; Rosenfeld, A.; Lazebnik, T. Multi-species prey–predator dynamics during a multi-strain pandemic. *Chaos an Interdisciplinary Journal of Nonlinear Science* **2023**, *33*.https://doi.org/10.1063/5.0154968
15. Pandey, V.; Singh, S. The analysis of global stability boundary and multistability in the nonlinear dynamical system of an advanced heavy water reactor. *Nuclear Science and Engineering* **2017**,*188*, 187–197. https://doi.org/10.1080/00295639.2017.1350003
16. Pandey, V.; Singh, S. Bifurcation analysis of the simplified models of boiling water reactor and identification of global stability boundary. *Nuclear Engineering and Design* **2017**, *315*, 93–103.https://doi.org/10.1016/j.nucengdes.2017.01.033
17. Pandey, V.; Singh, S. Bifurcation analysis of density wave oscillations in natural circulation loop. *International Journal of Thermal Sciences* **2017**, *120*, 446–458. https://doi.org/10.1016/j.ijthermalsci.2017.06.029

18. Pandey, V.; Singh, S. Detailed bifurcation analysis with a simplified model for advance heavy water reactor system. *Communications in Nonlinear Science and Numerical Simulation* **2015**, *20*, 186–198.https://doi.org/10.1016/j.cnsns.2014.05.019
19. Pandey, V.; Singh, S. Characterization of stability limits of Ledinegg instability and density wave oscillations for two-phase flow in natural circulation loops. *Chemical Engineering Science* **2017**, *168*, 204–224. https://doi.org/10.1016/j.ces.2017.04.041
20. Pandey, V.; Singh, S. Bifurcations emerging from a double Hopf bifurcation for a BWR. *Progress in Nuclear Energy* **2019**, *117*, 103049. https://doi.org/10.1016/j.pnucene.2019.103049
21. Djilali, S.; Cattani, C.; Guin, L. N. Delayed predator–prey model with prey social behavior. *the European Physical Journal Plus* **2021**, *136*. https://doi.org/10.1140/epjp/s13360-021-01940-9
22. Ajraldi, V.; Pittavino, M.; Venturino, E. Modeling herd behavior in population systems. *Nonlinear Analysis Real World Applications* **2011**, *12*, 2319–2338. https://doi.org/10.1016/j.nonrwa.2011.02.002
23. Venturino, E.; Petrovskii, S. Spatiotemporal behavior of a prey–predator system with a group defense for prey. *Ecological Complexity* **2013**, *14*, 37–47. https://doi.org/10.1016/j.ecocom.2013.01.004
24. Elena, E.; Grammauro, M.; Venturino, E.; Simos, T. E.; Psihoyios, G.; Tsitouras, C.; Anastassi, Z. Ecoepidemics with Two Strains: Diseased Prey. In Proceedings of the AIP Conference, 14 September 2011;. https://doi.org/10.1063/1.3637838
25. Elena, E.; Grammauro, M.; Venturino, E. Predator's alternative food sources do not support ecoepidemics with twostrains-diseased prey. *Network Biology* **2013**, *3*, 29–44.
26. Roman, F.; Rossotto, F.; Venturino, E. Ecoepidemics with two strains: diseased predators. *WSEAS Transactions on Biology and Biomedicine* **2011**, *8*, 73–85.
27. Bosica, C.; De Rossi, A.; Fatibene, N.L.; Sciarra, M.; Venturino, E. Two-strain ecoepidemic systems: the obligated mutualism case. *Applied Mathematics & Information Sciences* **2015**, *09*, 1677–1685. https://doi.org/10.12785/amis/090403
28. Cavoretto, R.; Collino, S.; Giardino, B.; Venturino, E. A two-strain ecoepidemic competition model. *Theoretical Ecology* **2014**, *8*, 37–52. https://doi.org/10.1007/s12080-014-0232-x
29. Banerjee, M.; Kooi, B.; Venturino, E. An Ecoepidemic Model with Prey Herd Behavior and Predator Feeding Saturation Response on Both Healthy and Diseased Prey. *Mathematical Modelling of Natural Phenomena* **2017**, *12*, 133–161. https://doi.org/10.1051/mmnp/201712208
30. Djilali, S. Impact of prey herd shape on the predator-prey interaction.*Chaos Solitons & Fractals* **2019**, *120*, 139–148. https://doi.org/10.1016/j.chaos.2019.01.022
31. Antwi-Fordjour, K.; Westmoreland, S.P.; Bearden, K.H. Dual fear phenomenon in an eco-epidemiological model with prey aggregation. *The European Physical Journal Plus* **2024**, *139*. https://doi.org/10.1140/epjp/s13360-024-05324-7
32. Kooi, B.W.; Venturino, E. Ecoepidemic predator–prey model with feeding satiation, prey herd behavior and abandoned infected prey. *Mathematical Biosciences* **2016**, *274*, 58–72. https://doi.org/10.1016/j.mbs.2016.02.003
33. Ruan, S.; Xiao, D.; Beier, J.C. On the Delayed Ross–Macdonald Model for Malaria Transmission. *Bulletin of Mathematical Biology* **2008**, *70*, 1098–1114. https://doi.org/10.1007/s11538-007-9292-z
34. Saha, S.; Samanta, G.P. Analysis of a predator–prey model with herd behavior and disease in prey incorporating prey refuge. *International Journal of Biomathematics* **2019**, *12*, 1950007. https://doi.org/10.1142/s1793524519500074
35. Venturino, E. The usefulness of mathematics in agriculture, for the environment and in contrasting diseases: insights from a wide range of simple models. *Communications in Applied and Industrial Mathematics* **2024**, *15*, 27–49. https://doi.org/10.2478/caim-2024-0002
36. Collino S.; Venturino E.; Ferreri L.; Bertolotti L.; Rosati S.; Giacobini M. Models for two strains of the Caprine Arthritis Encephalitis Virus Disease. In Biomat 2015, Mondaini, R.P.,Eds.; **2016**, 297–318.https://doi.org/10.1142/9789813141919_0019
37. Fournié, G.; Walker, P.; Porphyre, T.; Métras, R.; Pfeiffer, D. Mathematical Models of infectious diseases in livestock: Concepts and application to the spread of highly pathogenic Avian influenza virus strain type H5N1. In Springer eBooks **2011** 183–205. https://doi.org/10.1007/978-1-4419-7077-0_11
38. Doeschl-Wilson, A.; Knap, P.; Opriessnig, T.; More, S. Review: Livestock disease resilience: from individual to herd level. *Animal* **2021**, 15, 100286. https://doi.org/10.1016/j.animal.2021.100286

39. Mandal, D.S.; Samanta, S.; Alzahrani, A.K.; Chattopadhyay, J. STUDY OF a PREDATOR–PREY MODEL WITH PEST MANAGEMENT PERSPECTIVE. *Journal of Biological Systems* **2019**, *27*, 309–336. https://doi.org/10.1142/s021833901950013x https://doi.org/10.1140/epjp/s13360-021-01900-3
40. Verma, H.; Mishra, V.N.; Mathur, P. Effectiveness of lock down to curtail the spread of corona virus: A mathematical model. *ISA Transactions* **2022**, *124*, 124–134. https://doi.org/10.1016/j.isatra.2021.01.033
41. Mikheev, V.N.; Pasternak, A.F. Defense behavior of fish against predators and parasites. *Journal of Ichthyology* **2006**, *46*, S173–S179. https://doi.org/10.1134/s0032945206110063
42. Demandt, N.; Praetz, M.; Kurvers, R.H.J.M.; Krause, J.; Kurtz, J.; Scharsack, J.P. Parasite infection disrupts escape behaviours in fish shoals. In Proceedings of the Royal Society B Biological Sciences, 4 November 2020. https://doi.org/10.1098/rspb.2020.1158
43. Allan, B.J.M.; Illing, B.; Fakan, E.P.; Narvaez, P.; Grutter, A.S.; Sikkel, P.C.; McClure, E.C.; Rummer, J.L.; McCormick, M.I. Parasite infection directly impacts escape response and stress levels in fish. *Journal of Experimental Biology* **2020**. https://doi.org/10.1242/jeb.230904
44. Shi, Y.; Zhao, H.; Zhang, X. Dynamics of a multi-strain malaria model with diffusion in a periodic environment. *Journal of Biological Dynamics* **2022**, *16*, 766–815. https://doi.org/10.1080/17513758.2022.2144648
45. Roldan, J.A.M.; Otranto, D. Zoonotic parasites associated with predation by dogs and cats. *Parasites & Vectors* **2023**, *16*. https://doi.org/10.1186/s13071-023-05670-y
46. Lamichhane, B.; Mawad, A.M.M.; Saleh, M.; Kelley, W.G.; Harrington, P.J.; Lovestad, C.W.; Amezcua, J.; Sarhan, M.M.; Zowalaty, M.E.E.; Ramadan, H.; Morgan, M.; Helmy, Y.A. Salmonellosis: An overview of epidemiology, pathogenesis, and innovative approaches to mitigate the antimicrobial resistant infections. *Antibiotics* **2024**, *13*, 76. https://doi.org/10.3390/antibiotics13010076
47. Siddik, S.B.M.; Abdullah, F.A.; Ismail, A.I.M. Mathematical Model of Dengue Virus with Predator-Prey Interactions. *Sains Malaysiana* **2020**, *49*, 1191–1200. https://doi.org/10.17576/jsm-2020-4905-24
48. De Araújo, R.G.; Jorge, D.C.; Dorn, R.C.; Cruz-Pacheco, G.; Esteva, M.L.M.; Pinho, S.T. Applying a multi-strain dengue model to epidemics data. *Mathematical Biosciences* **2023**, 360, 109013. https://doi.org/10.1016/j.mbs.2023.109013
49. Ogunlade, S.T.; Adekunle, A.I.; McBryde, E.S.; Meehan, M.T. Modelling the ecological dynamics of mosquito populations with multiple co-circulating Wolbachia strains. *Scientific Reports* **2022**, *12*. https://doi.org/10.1038/s41598-022-25242-x
50. Xue, L.; Zhang, H.; Sun, W.; Scoglio, C. Transmission dynamics of multi-strain dengue virus with cross-immunity. *Applied Mathematics and Computation* **2021**, 392, 125742. https://doi.org/10.1016/j.amc.2020.125742
51. Martcheva, M. Evolutionary consequences of predation for pathogens in prey. *Bulletin of Mathematical Biology* **2009**, *71*, 819–844. https://doi.org/10.1007/s11538-008-9383-5
52. Dhooge, A.; Govaerts, W.; Kuznetsov, Y.A. MATCONT. *ACM Transactions on Mathematical Software* **2003**, *29*, 141–164. https://doi.org/10.1145/779359.779362